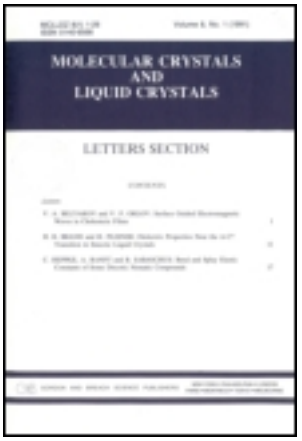


Molecular Crystals and Liquid Crystals
Publication details, including instructions for authors and subscription information:
http://www.tandfonline.com/loi/gmcl20

# Non-Doped Blue OLEDs Based on 9,9′-Dimethylfluorene Containing 10-Naphthylanthracene Derivatives

Eun Jae Na [a], Kum Hee Lee [a], Bo Young Kim [b], Seok Jae Lee [b], Young Kwan Kim [b] & Seung Soo Yoon [a]

[a] Department of Chemistry, Sungkyunkwan University, Suwon, 440-746, Korea

[b] Department of Information Display, Hongik University, Seoul, 121-791, Korea

Published online: 16 Dec 2013.

To cite this article: Eun Jae Na, Kum Hee Lee, Bo Young Kim, Seok Jae Lee, Young Kwan Kim & Seung Soo Yoon (2013) Non-Doped Blue OLEDs Based on 9,9′-Dimethylfluorene Containing 10-Naphthylanthracene Derivatives, Molecular Crystals and Liquid Crystals, 584:1, 113-122, DOI: 10.1080/15421406.2013.849466

To link to this article: http://dx.doi.org/10.1080/15421406.2013.849466

*Mol. Cryst. Liq. Cryst.*, Vol. 584: pp. 113–122, 2013

ISSN: 1542-1406 print/1563-5287 online
DOI: 10.1080/15421406.2013.849466

Taylor & Francis
Taylor & Francis Group

# Non-Doped Blue OLEDs Based on 9,9′-Dimethylfluorene Containing 10-Naphthylanthracene Derivatives

EUN JAE NA,[1] KUM HEE LEE,[1] BO YOUNG KIM,[2]
SEOK JAE LEE,[2] YOUNG KWAN KIM,[2]
AND SEUNG SOO YOON[1,*]

[1]Department of Chemistry, Sungkyunkwan University, Suwon 440-746, Korea
[2]Department of Information Display, Hongik University, Seoul 121-791, Korea



*A series of blue fluorescent materials **1–3** based on 10-(2-napthyl)-anthracene derivatives with the diverse aromatic groups were synthesized and multilayer non-doped devices using them as emitting materials were fabricated. All OLED devices using these materials emit deep blue light of 446–456 nm. In particular, device **3** exhibited highly efficient blue emissions with the luminous efficiency of 3.89 cd/A, a power efficiency of 2.47 lm/W, Quantum Efficiency of 3.03% at 20 mA/cm$^2$, and CIE*x,y *coordinates of (0.163, 0.149) at 6 V. Also, device 2 showed the efficient deep-blue emission with CIE coordinates of ($x = 0.151$, $y = 0.104$) at 6 V.*

**Keywords** Blue fluorescent materials; organic light-emitting diode; 10-naphthylanthracene derivative; Suzuki cross-coupling reaction.

## Introduction

Organic light-emitting devices (OLEDs) have been attracting considerable attention because of their potential application as flat-panel displays [1–2]. Among the three primary-color emitters (red, green and blue) in OLEDs, blue-light emitting materials are of particular importance because they are not only essential components for full-color display applications but also hosts for suitable lower-energy dopants to generate nearly all colors [3–6]. Recently, much effort has been devoted to developing new blue phosphorescent or fluorescent materials. However, blue phosphorescent materials are restricted to the instability and color saturation issues [7]. Therefore, deep-blue OLEDs mainly focus on fluorescent emitters, but only few of them have their device stabilities being mentioned [8–11].

Anthracene derivatives have been intensively studied for use as the blue emitting material in OLEDs, because these derivatives usually have excellent photoluminescence (PL) and electroluminescence (EL) properties, wide-energy gap, and good thermal stability [12–15]. Additionally, the emission of anthracene derivatives can be easily changed from blue to green by introducing symmetric or asymmetric moieties at the C-9 and C-10 positions [16].

*Address correspondence to Prof. Seung Soo Yoon, Department of Chemistry, Sungkyunkwan University, Cheoncheon-dong, Jangan-gu, Suwon, Gyeonggi-do, 440-746, Korea (ROK). Tel.: (+82)31-290-7071. Fax: (+82)31-290-7075. E-mail: ssyoon@skku.edu

In this study we have designed and synthesized three blue emitters based on 10-naphthylanthracene derivatives connected with the diverse aromatic groups. Fluorene, fluorenylphenyl, and phenylanthracenyl-fluorene groups were introduced to 9-position of the anthracene framework to increase steric hindrance and cause molecular non-planarity through twisting of the phenyl rings. The non-planarity of this molecular structure effectively diminishes its degree of intermolecular $\pi-\pi^*$ stacking and reduces self-quenching; meanwhile, the sterically bulky units facilitate the formation of stable amorphous films [17–18]. As will be seen below, in comparison with a common blue emitting material MADN, new host materials (**1–3**) provide the improved EL efficiencies due to their structural properties.

## Experimental

### *Synthesis*

9-(9,9-dimethylfluoren-2-yl)-10-(2-naphthyl)anthracene (1): 9-bromo-10-(naphthalen-2-yl)anthracene (1.19g, 3.12mmol) and 2-(9,9-dimethylfluoren-2-yl)-4,4,5,5-tetramethyl-1,3,2-dioxaborolane (1.20 g, 3.75 mmol), $Pd(PPh_3)_4$ (144 mg, 0.12 mmol), aqueous 2.0 M $K_2CO_3$ (4.13 g, 31.2 mmol), Aliquat 336 (0.14 ml, 0.31 mmol) and toluene (30 ml) were mixed in a flask. The mixture was refluxed at 120°C for 3 h. After the reaction had finished, the reaction mixture was extracted with Toluene and washed with water. The organic layer was dried with anhydrous $MgSO_4$ and filtered with silica gel. The solution was then evaporated. The crude product was purified recrystallization from $CH_2Cl_2$/EtOH. (1.17 g Yield: 94%) $^1$H-NMR (300 MHz, $CDCl_3$) [$\delta$ ppm]: 8.08 (d, $J = 8.4$ Hz, 1H), 8.03–7.98 (m, 2H), 7.96 (d, $J = 7.5$ Hz, 1H), 7.91 (d, $J = 2.7$ Hz, 1H), 7.85–7.81 (m, 3H), 7.75–7.71 (m, 2H), 7.63 (dd, $J = 1.8$, 3.6 Hz, 1H), 7.60–7.56 (m, 3H), 7.51–7.46 (m, 2H), 7.43–7.27 (m, 6H), 1.57 (s, 6H) $^{13}$C-NMR (75 MHz, $CDCl_3$) [$\delta$ ppm]: 154.2, 139.3, 138.8, 138.3, 138.1, 137.2, 136.9, 133.7, 133.1, 130.4, 129.7, 128.3, 128.2, 127.7, 127.5, 126.5, 126.3, 125.9, 125.7, 125.4, 125.1, 123.3, 122.8, 120.5, 120.2, 47.3, 27.7, 27.4 FT-IR [ATR]: $\nu$ 3057, 2961, 1602, 1514, 1442, 1267, 758, 738 cm$^{-1}$. MS (EI$^+$) m/z 497(M$^+$).

9-(4-(9,9-dimethylfluoren-2-yl)phenyl)-10-(2-naphthyl)anthracene (2): 9-bromo-10-(naphthalen-2-yl)anthracene (500mg, 1.30mmol) and 2-(4-(9,9-dimethylfluoren-2-yl)phenyl)-4,4,5,5-tetramethyl-1,3,2-dioxaborolane (620 g, 1.56 mmol), $Pd(PPh_3)_4$ (60.3 mg, 0.05 mmol), aqueous 2.0 M $K_2CO_3$ (1.79 g, 13.0 mmol), Aliquet 336 (0.05 ml, 0.13 mmol) and toluene (17 ml) were mixed in a flask. The mixture was refluxed at 140°C for 8 h. After the reaction had finished, the reaction mixture was extracted with Toluene and washed with water. The organic layer was dried with anhydrous $MgSO_4$ and filtered with silica gel. The solution was then evaporated. The crude product was purified recrystallization from $CH_2Cl_2$/EtOH. (560mg Yield: 75%) $^1$H-NMR (300 MHz, $CDCl_3$) [$\delta$ ppm]: 8.09 (d, $J = 8.4$ Hz, 1H), 8.03–7.99 (m, 2H), 7.93 (d, $J = 8.1$ Hz, 3H), 7.87 (t, $J = 7.8$ Hz, 4H), 7.80–7.72 (m, 4H), 7.63–7.57 (m, 5H), 7.49 (dd, $J = 1.8$, 6.6 Hz, 1H), 7.38–7.31 (m, 6H) 1.60 (s, 6H) $^{13}$C-NMR (75 MHz, $CDCl_3$) [$\delta$ ppm]: 154.7, 154.2, 141.0, 140.3, 139.2, 139.0, 138.2, 137.3, 137.3, 136.9, 133.7, 133.1, 132.1, 130.5, 130.4, 130.3, 129.9, 128.4, 128.3, 128.2, 127.6, 127.5, 127.4, 126.7, 126.5, 125.5, 125.4, 123.0, 121.7, 120.7, 120.4, 47.3, 27.6 FT-IR [ATR]: $\nu$ 2968, 2867, 1739, 1444, 1389, 1364, 1225, 1056, 1030, 823, 778 cm$^{-1}$. MS (EI$^+$) m/z 573 (M$^+$).

9-(9,9-dimethyl-7-(10-(2-naphthyl)anthracen-9-yl)-fluoren-2-yl)-10-phenylanthracene(3): 9-(7-bromo-9,9-dimethylfluoren-2-yl)-10-phenylanthracene (535 mg, 1.01 mmol) and 10-(naphthalen-2-yl)anthracen-9-ylboronic acid (425 g, 1.22 mmol), $Pd(PPh_3)_4$

(47.0 mg, 0.04 mmol), aqueous 2.0 M $Na_2CO_3$ (1.07 g, 10.1 mmol), EtOH (5 ml) and toluene (15 ml) were mixed in a flask. The mixture was refluxed at 120°C for 3 h. After the reaction had finished, the reaction mixture was solid filter and washed with water. The solid melted with hot toluene and then dried with anhydrous $MgSO_4$ and filtered with silica gel. The solution was then evaporated. The crude product was purified recrystallization from $CH_2Cl_2$/Hexane. (648 mg Yield: 85%) $^1$H-NMR (300 MHz, $CDCl_3$) [$\delta$ ppm]: 8.10 (d, $J$ = 7.8 Hz, 3H), 8.05–8.00 (m, 3H), 7.95–7.92 (m, 1H), 7.89 (t, $J$ = 8.1 Hz, 4H), 7.77 (m, 4H), 7.66–7.49 (m, 12H), 7.41–7.31 (m, 7H), 1.65 (s, 6H) $^{13}$C-NMR (75 MHz, $CDCl_3$) [$\delta$ ppm]: 154.5, 139.4, 138.7, 138.5, 137.9, 133.7, 131.6, 130.7, 130.5, 130.4, 130.4, 130.3, 130.3, 129.9, 128.7, 128.4, 128.3, 128.2, 127.4, 127.4, 126.7, 126.5, 126.2, 125.4, 120.3, 47.6, 27.7 FT-IR [ATR]: $\nu$ 2971, 2868, 1739, 1374, 1218, 1056, 1031, 769 cm$^{-1}$. MS (EI$^+$) m/z 748 (M$^+$).

### *Fabrication of OLED*

For fabricating OLEDs, indium-tin-oxide (ITO) thin films coated on glass substrates were used, which was 30 square of the sheet resistivity, and 100 nm of thickness. The ITO-coated glass was cleaned in an ultrasonic bath by the following sequence: acetone, methyl alcohol, distilled water, and stored in isopropyl alcohol for 48 h and dried by a $N_2$ gas gun. The substrates were treated by $O_2$ plasma under $2.0 \times 10^{-2}$ torr at 125 W for 2 min. All organic materials and metals were deposited under high vacuum ($5 \times 10^{-7}$ torr). The OLEDs were fabricated in the following sequence: ITO/4,4′-Bis(N-(1-naphthyl)-N-phenylamino)biphenyl (NPB) (50 nm)/Blue emitting materials (**1–3**) (30 nm)/4,7-Diphenyl-1,10-phenanthroline (Bphen) (30 nm)/Lithium quinolate (Liq) (2 nm)/Al (100 nm), NPB as the hole-transporting layer, Bphen as the electron-transporting layer, and Liq:Al as the composite cathode. The current density ($J$), luminance (L), luminous efficiency (LE), and CIE chromaticity coordinates of the OLEDs were measured with a Keithly 2400, Chroma meter CS-1000A. Electroluminance was measured using a Roper Scientific Pro 300i.

### *Measurements*

$^1$H- and $^{13}$C-NMR were recorded on a Varian Unity Inova 300Nb spectrometer. FT-IR spectra were recorded using a Bruker VERTEX70 FT-IR spectrometer. Low- resolution mass spectra were measured using a Jeol JMS-600 spectrometer in the EI mode. The UV-Vis absorption and photoluminescence spectra of the new host materials were measured in dichloromethane ($10^{-5}$ M) using Shimadzu UV-1650PC and Amincobrowman series 2 luminescence spectrometers. The fluorescence quantum yields of the emitting materials were determined in dichloromethane at 293 K against DPA(9,10-diphenylanthracene) as a reference ($\Phi_{DPA} = 0.90$). The HOMO (highest occupied molecular orbital) energy levels were measured with a low-energy photoelectron spectrometer (Riken-Keiki, AC-2). The energy band gaps were determined from the intersection of the absorption and photoluminescence spectra. LUMO (lowest unoccupied molecular orbital) energy levels were calculated by subtracting the corresponding optical band gap energies from the HOMO energy values.

## Results and Discussion

Scheme 1 shows the synthesis and structures of the designed blue fluorescent materials. Suzuki cross-coupling reactions between the 9-(2-naphthalene)-anthracene-10-boronic acid

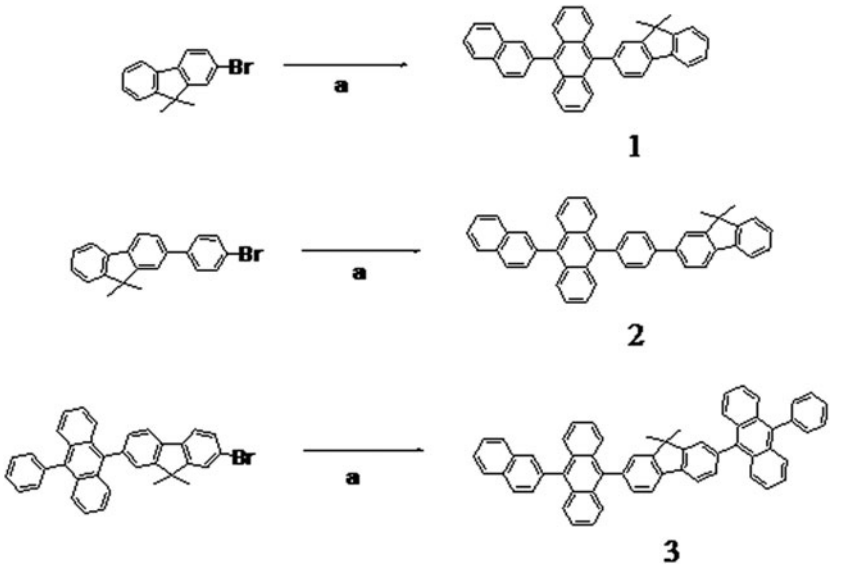


**Scheme 1.** Synthesis of new host materials (**1–3**). (a) 9-(2-Naphthalene)-Anthracene-10-boronic acid, $Pd(PPh_3)_4$, 2M $Na_2CO_3$, Toluene/EtOH, reflux, 4 h.

and the corresponding aryl bromides afforded the blue-emitting materials (**1–3**) in moderate yields. After the conventional purifications such as column chromatography and recrystallization, these newly synthesized blue-emitting materials (**1–3**) were fully characterized with $^1$H- and $^{13}$C-NMR, and mass spectroscopy.

Figure 1 presents the UV-vis absorption and PL emission spectra of blue fluorescent materials **1–3** in dichloromethane solutions and on quartz plate films. The absorption spectra of the compounds in $CH_2Cl_2$ solution show the characteristic vibronic band from the $\pi-\pi^*$ transitions of the isolated anthracene group ($\lambda_{max}$ are about 378, 377 and 378 nm) [19–20]. As summarized in Table 1, all host materials (**1–3**) showed identical blue fluorescence with maximum emission wavelengths at 430 nm, furthermore, these compound (**1–3**) had more deep-blue maximum emission peaks than the common host material MADN maximum emission peaks at 436 nm. The band-gap energy of the blue fluorescent materials (**1–3**) ranged from 3.05 to 3.08 eV, which was wider than the 3.0 eV of the MADN. Compared to solution states, the PL spectral bathochromic shift in solid state is due to

**Table 1.** Optical properties of new host materials **(1–3)**

| Compound | $UV_{max}$ [nm][a] | $PL_{max}$ [a] [nm] | $PL_{max}$ [b] [nm] | FWHM [nm] | HOMO/LUMO [eV] | $E_g$ [eV] | $\Phi$ [%][c] |
|---|---|---|---|---|---|---|---|
| 1 | 360,378,398 | 430 | 453 | 54 | −5.80/−2.73 | 3.07 | 0.53 |
| 2 | 358,377,397 | 430 | 448 | 54 | −5.83/−2.75 | 3.08 | 0.63 |
| 3 | 359,378,399 | 430 | 449 | 52 | −5.81/−2.76 | 3.05 | 0.47 |
| MADN | 398 | 436 | 447 | 60 | −5.50/−2.50 | 3.0 | 0.54 |

[a]$CH_2Cl_2$ solution ($10^{-5}$ M). [b]Thin film. [c]Using 9,10-diphenylanthracene as a standard; $\lambda_{ex}$ = 360 nm ($\Phi = 0.90$ in $CH_2Cl_2$). Ref. 21.

**Table 2.** EL performance characteristic of the devices **(1–3)** (non-doped)

| Device | $\lambda_{,max}^{EL}$, FWHM[a] [nm] | $L$[b] [cd/m$^2$] | $J$[b] [mA/cm$^2$] | LE[c,d] [cd/A] | PE[c,d] [lm/W] | EQE[c,d] [%] | CIE[e] ($x$,$y$) |
|---|---|---|---|---|---|---|---|
| 1 | 446, 65 | 1207 | 217 | 1.14/1.13 | 1.70/0.76 | 0.88/0.87 | (0.173,0.154) |
| 2 | 449, 56 | 2559 | 156 | 2.65/2.38 | 2.77/1.58 | 2.72/2.53 | (0.151,0.104) |
| 3 | 456, 61 | 4454 | 213 | 3.95/3.89 | 3.67/2.47 | 3.03/3.03 | (0.163,0.149) |
| MADN | 442, 55 | 954 | 154 | 1.35/1.08 | 1.01/0.48 | 1.45/0.98 | (0.153,0.080) |

[a]Emission maximum and FWHM of EL emission spectra. [b]Maximum luminance and current density. [c]Maximum values. [d]At 20 mA/cm$^2$. [e]Commission Internationale d'Énclairage (CIE) at 6.0 V.



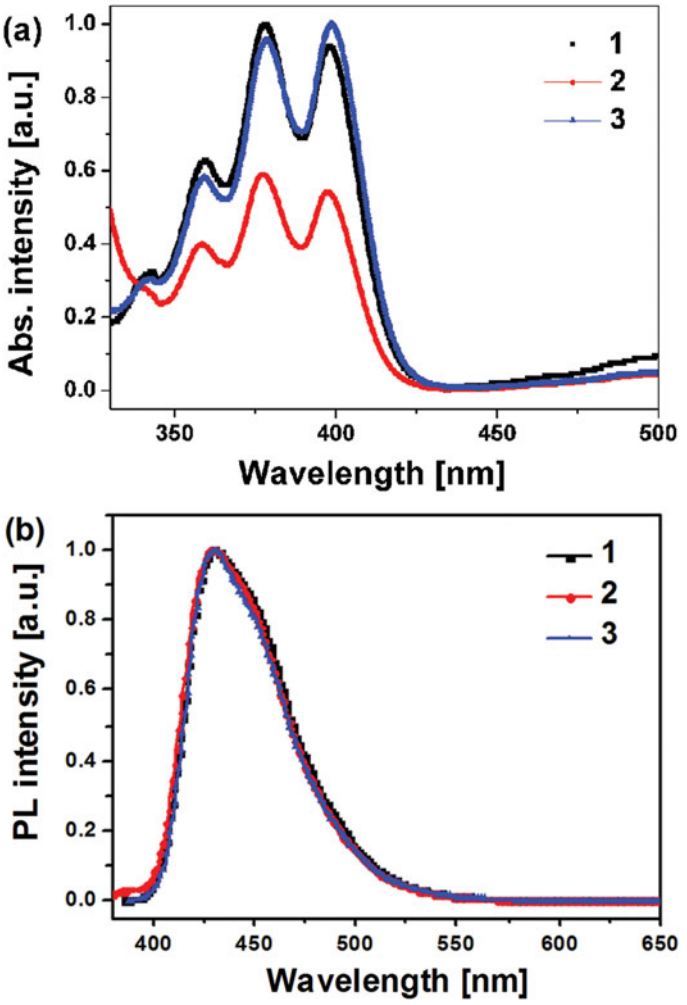


**Figure 1.** (a) The absorption spectra and (b) emission spectra of the host materials (**1–3**).

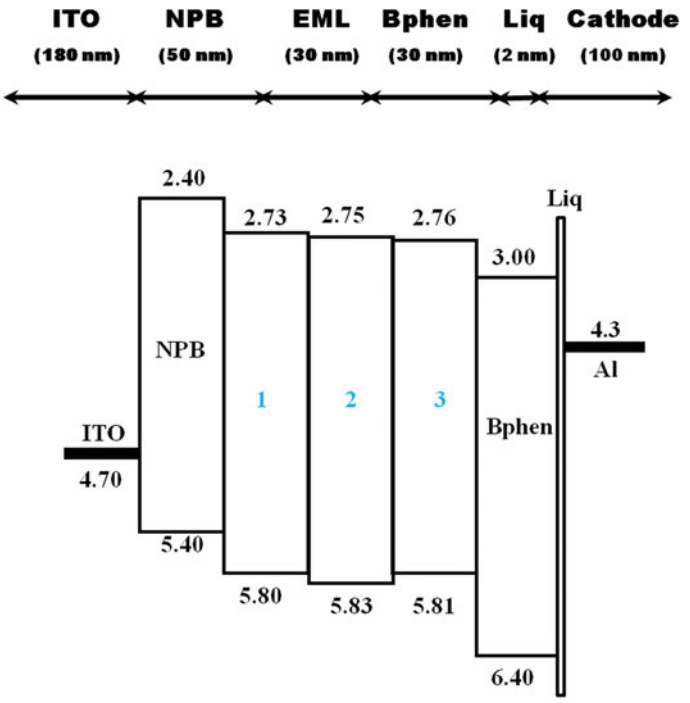


**Figure 2.** Energy levels diagram of compounds **(1–3)** used in the OLED fabrication.

the self-aggregation by intermolecular interactions between materials **1–3**. Interestingly, compared to the PL spectrum of compound **2** (ca. 18 nm) and **3** (ca. 19 nm), that of compound **1** shows more a red shift (ca. 23 nm) in film state. This is because compound **1** had more planar structure than compounds **2** and **3,** which is imply that the bulky and

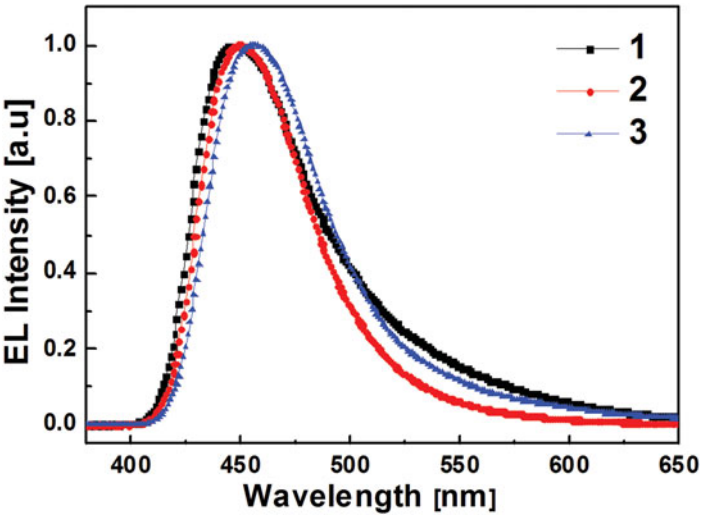


**Figure 3.** EL spectra of devices **1–3**.

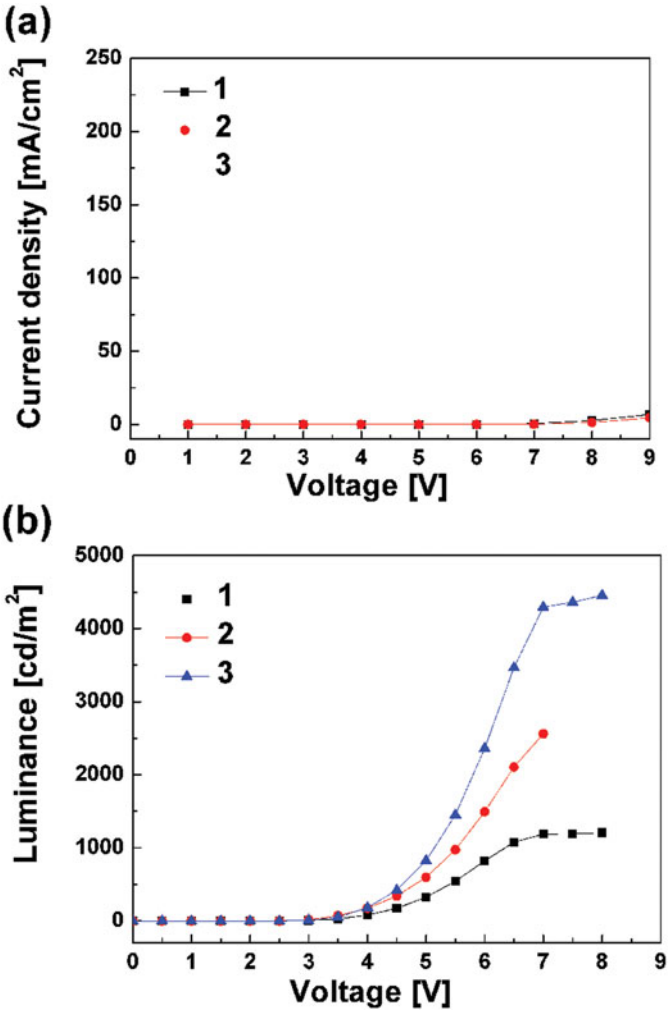


**Figure 4.** (a) Current density and (b) luminance versus applied electric voltage characteristics of devices **1–3**.

non-coplanar end-capped groups of compounds **2** and **3** effectively suppress intermolecular interaction in solid state. Furthermore, compared to the FWHM of MADN (60 nm), FWHM of compound **1–3** exhibited very narrow in the range from 52 nm to 54 nm. It suggests that the intermolecular interactions of the compound **1–3** are weaker than those of MADN. The fluorescence quantum yields ($\Phi_f$) of the anthracene derivatives in dilute dichloromethane solution were measured by using 9,10-diphenylanthracene ($\Phi_{DPA} = 0.90$) as the reference material [21]. These deep-blue emitters **1–3** show good quantum yields of 0.53, 0.63, and 0.47, suggesting that these materials are expected to have highly efficient electroluminescent properties in OLED devices.

To investigate the electroluminescence (EL) performance of the new blue emitting materials (**1–3**), we fabricated non-doped devices with a configuration of ITO (180 nm)/NPB (50 nm)/Blue emitting materials (**1–3**) (30 nm)/Bphen (30 nm)/Liq (2 nm)/Al (100 nm), NPB is used as the hole-transporting layer, Bphen as the electron-transporting layer, and

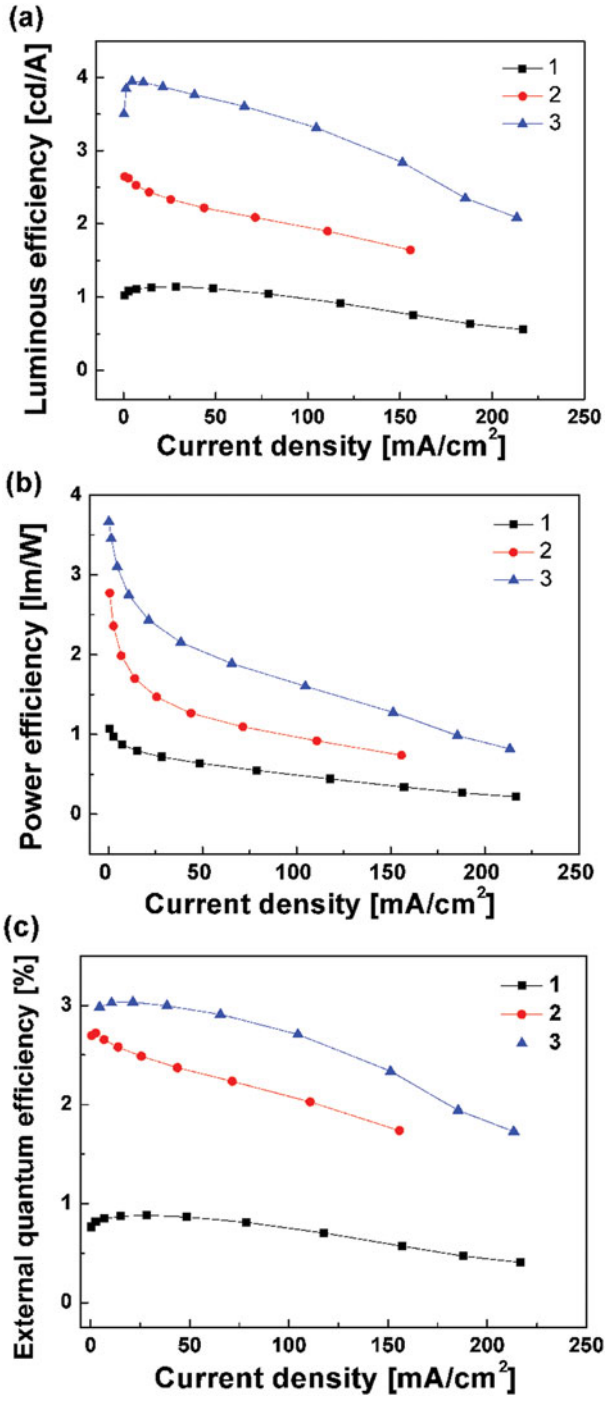


**Figure 5.** (a) Luminous, (b) power and (c) external quantum efficiencies as a function of current density for devices **1–3**.

Liq:Al as the composite cathode. The EL properties of devices **1–3** are summarized in Table 2, with all devices showing low turn-on voltages no greater than 2.6 V. One important reason for such low turn-on voltages is the ambipolar transporting property of the anthracene derivatives [18]. Also, the small injection barriers in the devices would partially contribute to the low turn-on voltages of devices **1–3**, as shown in HOMO-LUMO energy level diagram of these OLEDs in Fig. 2. The hole injection barrier at the NPB/anthracene junction is about 0.4 eV, and the electron injection barrier at the anthracene derivatives/Bphen junction is about 0.3 eV. These small injection barriers enhance injection efficiency of both holes and electrons into the emission layer.

Figure 3 shows the normalized EL spectra of the three devices, these EL emission maxima of the devices are in the range of 446–456 nm, exhibiting small blue-shifts relative to the PL spectra from the thin film samples. Narrow EL peaks with FWHMs of 65, 56 and 61 nm were respectively observed in the **1–3** based devices. At a driving voltage of 6V, the CIE coordinates of devices **1–3** were (0.173, 0.154), (0.151, 0.104), and (0.163, 0.149), respectively. These high color purity of blue emissions confirm that the non-coplanar molecular structures of the three compounds can effectually hinder intermolecular aggregation. Particularly, device **2** gives more saturated NTSC standard blue color (0.14, 0.08) in comparison to **1** and **3**. Presumably, compound **2** has the increased steric hindrance due to the twisting of the phenyl ring and thus causes the more molecular nonplanarity in comparison to **1** and **3**. This structure prevents close molecular packing in the solid state and also effectively suppresses excimer or exciplex formations and fluorescence quenching.

Figure 4 presents the *luminance-voltage* and *current density-voltage* characteristics of the non-doped devices. The maximum brightness of the anthracene-based blue OLEDs varied from 1207 cd $m^{-2}$ in device **1** to as high as 4454 cd $m^{-2}$ in device **3**. Presumably, device **3** with double-anthracene end-capping groups gave the best device luminance among the devices. Notably, luminance of devices **1–3** have presented at the lowest about 1.3 fold to at the most fivefold increase over those of device using MADN.

The luminous and power efficiencies and external quantum efficiency of devices **1–3**, as a function of the current density, are shown in Fig. 5. The maximum luminous efficiencies were 1.14, 2.65 and 3.95 cd/A at 20 mA/$cm^2$, maximum power efficiencies of 1.70, 2.77, and 3.67 lm/W, and maximum external quantum efficiencies 0.88, 2.72 and 3.03% respectively. On the whole of EL performance, devices **1–3** showed improved luminous efficiencies, power efficiencies and external quantum efficiencies compared to the device using a common blue emitting material MADN. This study clearly suggests that the emitting materials **1–3** has the excellent properties for blue OLEDs.

## Conclusions

A series of asymmetric anthracene derivatives **1–3**, based on 10-(2-napthyl)-anthracene, were synthesized and characterized. All OLED devices using compounds **1–3**, showed the efficient deep blue emissions with the EL maximum at 446–456 nm. In particular, device **3** exhibited highly efficient blue emissions with the luminous efficiency of 3.89 cd/A, a power efficiency of 2.47 lm/W, Quantum Efficiency of 3.03% at 20 mA/$cm^2$, and CIE*x,y* coordinates of (0.163, 0.149) at 6 V. Also, device **2** showed the efficient deep-blue emission with CIE coordinates of (0.151, 0.104) at 6 V.

## Acknowledgment

This research (S2012-0870-000) was supported by the MKE (The Ministry of Knowledge Economy), Korea, under the ITRC (Information Technology Research Center)/CITRC (Convergence Information Technology Research Center) support program (NIPA-2012-H0301-12-4013) supervised by the NIPA (National IT Industry Promotion Agency).

## References

[1] Sun, Y. R., Giebink, N. C., Kanno, H., Na, B. W., Thompson, M. E., & Forrest, S. R. (2006). *Nature*, *440*, 908.
[2] Tang, C. W., Vanslyke, S. A., & Chen, C. H. (1989). *J. Appl. Phys.*, *65*, 3610.
[3] Mitschke, U., & Bauerle, P. (2000). *J. Mater. Chem.*, *10*, 1047.
[4] Park, J. K., Lee, K. H., Kang, S., Lee, J. Y., Park, J. S., Seo, J. H., Kim, Y. K., & Yoon, S. S. (2010). *Org. Electron.*, *11*, 905.
[5] Lee, K. H., Kwon, Y. S., Lee, J. Y., Kang, S., Yook, K. S., Jeon, S. O., Lee, J. Y., & Yoon, S. S. (2011). *Chem. Eur. J.*, *17*, 12994.
[6] Lee, K. H., Kang, L. K., Kwon, Y. S., Lee, J. Y., Kang, S., Kim, G. Y., Seo, J. H., Kim, Y. K., & Yoon, S. S. (2010). *Thin Solid Films*, *518*, 5091.
[7] Lee, K. H., Kwon, Y. S., Kang, L. K., Kim, G. Y., Seo, J. H., Kim, Y. K., & Yoon, S. S. (2009). *Synthetic Metals*, *159*, 2603.
[8] Kim, S. O., Lee, K. H., Kang, S., Lee, J. Y., Seo, J. H., Kim, Y. K., & Yoon, S. S. (2010). *Bull. Korean Chem. Soc.*, *31*, 389.
[9] Lee, K. H., Kim, S. O., You, J. N., Kang, S., Lee, J. Y., Yook, K. S., Jeon, S. O., Lee, J. Y., & Yoon, S. S. (2012). *J. Mater. Chem.*, *22*, 5145.
[10] Kim, K. S., Lee, H. S., Joen, Y. M., Kim, J. W., & Lee, C. W. (2009). *Dyes and Pigments*, *81*, 174.
[11] Lee, K. H., Kang, L. K., Lee, J. Y., Kang, S., Jeon, S. O., Yook, K. S., Lee, J. Y., & Yoon, S. S. (2010). *Adv. Funct. Mater.*, *20*, 1345.
[12] Oh, S. H., Lee, K. H., Seo, S. H., Kim, Y. K., & Yoon, S. S. (2011). *Bull. Korean Chem. Soc.*, *32*, 1593.
[13] Park, J. K., Lee, K. H., Park, J. S., Seo, J. H., Kim, Y. K., & Yoon, S. S. (2011). *J. Nanosci. Nanotechnol.*, *11*, 4359.
[14] Lee, K. H., Park, J. K., Seo, J. H., Park, S., Kim, Y. S., Kim, Y. K., & Yoon, S. S. (2011). *J. Mater. Chem.*, *21*, 13640.
[15] Lee, K. H., Son, C. S., Lee, J. Y., Kang, S., Yook, K. S., Jeon, S. O., Lee, J. Y., & Yoon, S. S. (2011). *Eur. J. Org. Chem.*, *4788*.
[16] Suk, J. D., Wu, Z., Wang, L., & Bard, A. J. (2011). *J. Am. Chem. Soc.*, *133*, 14675.
[17] Shih, P. I., Chuang, C. Y., Chien, C. H., Diau, E. W. G & Shu, C. F. (2007). *Adv. Funct. Mater.*, *17*, 3141.
[18] Zheng, C. J., Zhao, W. M., Wang, Z. Q., Huang, D., Ye, J., Ou, X. M., Zhang, X. H., Lee, C. S., & Lee, S. T. (2010). *J. Mater. Chem.*, *20*, 1560.
[19] Kim, S. O., Lee, K. H., Kim, G. Y., Seo, J. H., Kim, Y. K., & Yoon, S. S. (2010). *Synthetic Metals*, *160*, 1259.
[20] Bin, J. K., & Hong, J. I. (2011). *Org. Electron.*, *12*, 802.
[21] Wen, S. W., Lee, M. T., & Chen, C. H. (2005). *J. Display Technol.*, *1*, 90.